Effect of Pulsed Power on Particle Matter in Diesel Engine Exhaust using a DBD Plasma Reactor

Meisam Babaie, Pooya Davari, *Member*, *IEEE*, Firuz Zare, *Senior Member*, *IEEE*, MD Mostafizur Rahman, Hassan Rahimzadeh, Zoran Ristovski, and Richard Brown

***Abstract*— Non-thermal plasma (NTP) treatment of exhaust gas is a promising technology for both nitrogen oxides (NO_X) and particulate matter (PM) reduction by introducing plasma into the exhaust gases. This study considers the effect of NTP on PM mass reduction, PM size distribution and PM removal efficiency. The experiments have been performed on real exhaust gases from a diesel engine. The NTP is generated by applying high voltage pulses using a pulsed power supply across a dielectric barrier discharge (DBD) reactor. The effects of the applied high voltage pulses up to 19.44kVpp with repetition rate of 10 kHz are investigated. In this paper, it is shown that PM removal and PM size distribution need to be considered both together, as it is possible to achieve high PM removal efficiency with undesirable increase in the number of small particles. Regarding these two important factors, in this research, 17kVpp voltage level is determined to be an optimum point for the given configuration. Moreover, particles deposition on the surface of the DBD reactor was found to be a significant phenomenon which should be considered in all plasma PM removal tests.**

***Index Terms*—Particle size distribution, particle mass reduction, diesel exhaust gas, dielectric barrier discharge (DBD), pulsed power, push-pull converter.**

I. INTRODUCTION

There is a continuous increase in the number of diesel engines in both stationary and mobile application due to the lower operating cost, higher thermal efficiency, longer durability as well as lower hydrocarbons (HC) and carbon monoxide (CO) emissions [1]. However NO_X and particulate matter (PM) emissions still remain the two main environmental concerns in diesel engine applications. Studies focused on risk assessment have showed that high outdoor NO_X concentration observed in residential areas contributes to increased respiratory and cardiovascular diseases and mortality [2]. Moreover, the health effects of diesel particulate matter have been an area of concern for many years, due to both the chemical composition and the particle size distribution [3]. The small particles are inhalable and penetrate deep into the lungs where they are able to enter the bloodstream and even reach the brain [4, 5].

Up to now, several technologies have been applied for NO_X and particulate treatment of diesel engines. In recent years, application of non-thermal plasma (NTP) in exhaust gas treatment has gained lot of interests [6-9]. NTP treatment of exhaust gas is a promising technology for both NO_X and PM reduction by introducing plasma inside the exhaust gases. In the non-thermal plasma, electrons have a kinetic energy higher than the energy corresponding to the random motion of the background gas molecules. The intent of using non-thermal plasma is to selectively transfer the input electrical energy to the electrons which would generate free radicals through collisions and promote the desired chemical changes in the exhaust gas. These reactions can be accomplished at a fraction of the energy which is required in a thermal plasma system [10]. NO_X, unburned hydrocarbons, CO, and PM will be oxidized due to oxidation processes which happen by introducing plasma in the exhaust gas.

Applying pulsed power is one of the efficient ways to generate NTP. Pulsed power is the rapid release of stored energy in the form of electrical pulses into a load, which can result in delivery of large amounts of instantaneous power over a short period of time. Recently, solid-state pulsed power has gained more interest as it is compact, reliable, has a long lifetime and high repetition rate. In the last decade, research and studies established the advantage of using power electronics topologies in pulsed power applications [11-13]. In this research a bipolar pulsed power supply based on push-pull topology is implemented.

Generally, a pulsed power supply is employed to generate NTP using a dielectric barrier discharge (DBD) reactor. A DBD is essentially a multilayer capacitor which has been extensively used for various applications [14-21]. Also it can be a packed bed DBD reactor

[22-29] or assisted by another catalyst or adsorbent [22, 28, 30-37]. Here, a conventional DBD reactor with multipoint-to-plane geometry is developed.

Diesel particulate matter (DPM) consist mostly of carbonaceous soot with minor components of volatile organic fraction (VOF) from unburned fuel, lubricating oil, inorganic compounds such as ash and sulphur compounds and metals including zinc from lubricating oil [38]. DPM are the cause of a series of adverse effects on environment [39] and human health [40-42]. Particulate formation begins with nucleation in the engine cylinder and dilution tunnel, and is followed thereafter by agglomeration [43]. Most of the diesel particulate matter mass is in the accumulation mode, whereas in terms of particle number, most particles are found in the nucleation mode. More than 90% of diesel exhaust-derived PM is smaller than 1 μm in diameter [44]. Most of the mass is in the 0.1–1.0 μm "accumulation" size fraction, while most of the particle numbers are in the <0.1 μm "nano-particle" fraction [45, 46]. Ultrafine particles have an aerodynamic diameter less than 100 nm and are emitted in high number by compression ignition engines. Whilst ultrafine particles do not contribute much to the total mass of particulate matter emitted from an engine, they contribute greatly to the total number of particles. The particle size distribution of particulate matter from compression ignition engines has become of increased concern since a study by the Health Effects Institute demonstrated an increased number of nanoparticles emitted from a 1991 Cummins engine, despite a reduction in overall particle mass, relative to an older 1988 Cummins engine [47].

Ultrafine particles can penetrate deep into the lungs where they are able to enter the bloodstream and even reach the brain [4]. The respiratory health effects (in particular asthma) from particle emissions correlate strongly with particle number, rather than particle mass emissions [48] . In 2014 the Euro VI regulation will be implemented and the number of particles emitted by compression ignition engines (in addition to a new particle mass limit) will be regulated. This demonstrates that particle number emissions are becoming a very prominent issue in engine design and research [49, 50].

The main concern of this paper is to analyse the effect of pulsed power on PM mass reduction and PM size distribution considering the pulsed power effects on ultra-fine particles emitted from real diesel engine exhaust gas. In this research, a pulsed power supply based on the push-pull inverter is developed to generate up to 19.44kVpp across the DBD load. The experiments were conducted at different voltage levels with fixed repetition rate of 10 kHz. PM mass reduction, PM removal efficiency and PM size distribution are investigated by evaluating the results obtained.

II. EXPERIMENTAL METHOD

A. Experimental Setup

A schematic diagram of the experimental setup is shown in Fig. 1. Experiments were conducted on a modern turbo-charged 6-cylinder Cummins diesel engine (ISBe22031) at the Queensland University of Technology (QUT) Biofuel Engine Research Facility (BERF). The engine has a capacity of 5.9l, a bore of 102 mm, a stroke length of 120 mm, a compression ratio of 17.3:1 and maximum power of 162 kW at 2500 rpm. Particle number distributions are measured with a scanning mobility particle sizer (SMPS) consisting of a TSI 3080 classifier, which pre-selects particles within a narrow mobility (and hence size) range and a TSI 3025 condensation particle counter (CPC) which grows particles (via condensation) to optically detectable sizes. The SMPS software increases the classifier voltage in a pre-determined manner so that particles within a 10-500 nm size range are pre-selected and subsequently counted using the CPC. The software also integrates the particle number distribution to enable calculation of the total number of particles emitted by the engine at each test mode. Gaseous emissions are measured with CAI 600 series gas analyses. CO_2, NO_X and CO concentrations can be measured by this gas analyser, whereas particulate mass emissions are measured with a TSI 8530 Dust-Track II.

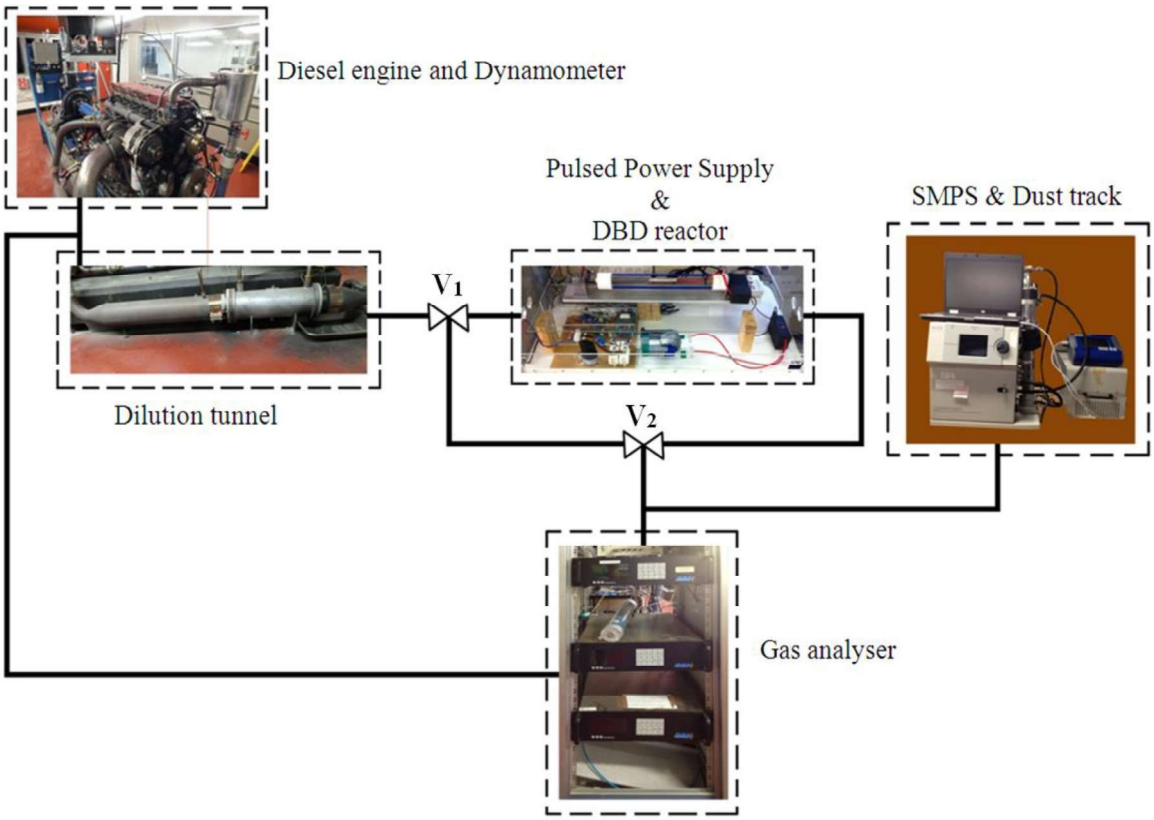

Fig. 1. Schematic diagram of plasma treatment system developed at QUT engine lab.

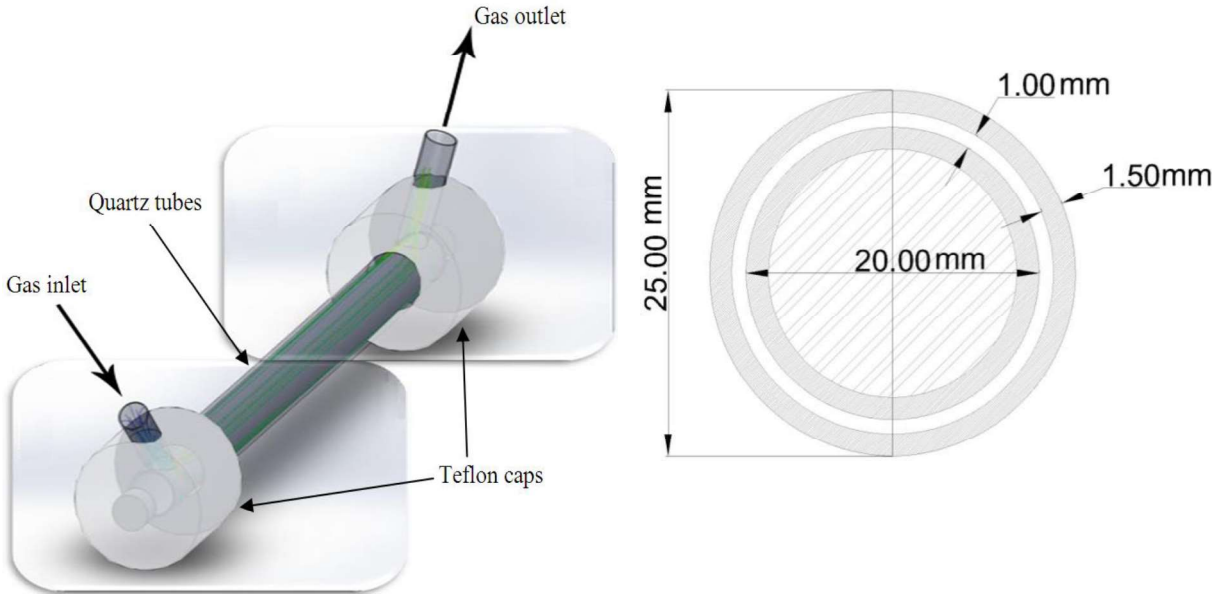

Fig. 2. DBD reactor in Solidworks: a) schematic, b) cross-section.

As depicted in Fig. 1, three way valves to control the exhaust gas path ways are employed. With this configuration, it is possible to measure both gaseous emissions and particles before entering the reactor and after leaving it by changing the three way valve directions. CO_2 was used as a tracer gas in order to calculate the dilution ratio. CO_2 was measured from the dilution tunnel with dilution ratios being calculated using the following equation:

$$Dilution ratio = \frac{CO_{2,exhaust} - CO_{2,background}}{CO_{2,diluted} - CO_{2,background}} \quad (1)$$

Laboratory background CO_2 measurements were made before the commencement of each test session. Every concentration measured after dilution should be modified by using the dilution ratio.

B. DBD Reactor

A conventional dielectric barrier discharge reactor was designed for the experiments. Fig. 2 shows a schematic of the reactor. As illustrated in Fig. 2, it consists of two concentric quartz tubes. Both tubes are 400 mm long and have a wall thickness of 1.5 mm. The outside diameters of inner and outer quartz tubes are 20mm and 25mm, respectively. Exhaust gas passes through the gap between these two quartz tubes. Based on pre-designed geometry, the discharge gap is 1 mm. The DBD is connected to the pulsed power supply using internal and external electrodes. The internal electrode is a copper cylinder and the external electrode is made by a copper mesh that wraps the exterior part of the DBD. The electrodes are placed in

the middle of the DBD load with the length of 100 mm. Both tubes are fixed by two Teflon caps at each end. Exhaust enters the reactor at the angle of 45 degree and flows throughout the gap and leaves the reactor with the same angle.

C. Bipolar Pulsed Power Supply

Fig. 3 shows a circuit schematic diagram of the pulsed power supply. As illustrated, it is based on the push-pull inverter topology. The push-pull inverter contains two switches that are driven with respect to ground. This is the main advantage of the inverter. This topology uses a centre-tapped transformer which is excited in both directions. A step up transformer is used to boost the voltage and achieve galvanic isolation.

The main reason to use a push-pull topology is to generate bipolar output voltage. Applying voltage periodically build-up charges across the electrodes, which can results in arcing. In order to sustained non-thermal plasma and prevent from arcing, bipolar pulse generation can employed for clearing charges [50]. Employing lower number of switches is another advantage of push-pull inverter. The two switches S_1 and S_2 are switched alternately with a controlled duty ratio to convert input DC voltage into high frequency AC voltage suitable for exciting the DBD load. Hence, the generated output voltage is bipolar.

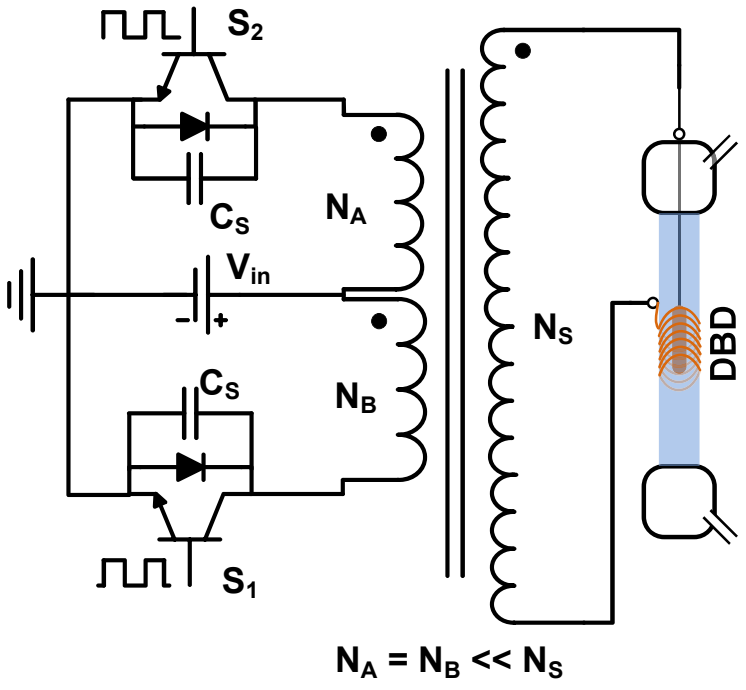

Fig. 3. Pulsed power supply circuit schematic diagram (push-pull inverter)

Adding a DBD load turns the push-pull inverter into a resonant stage with approximately sinusoidal output. The frequency of the semi-sinusoidal shape signal is determined by an L-C circuit comprising of the transformer inductance and capacitances of DBD and the transformer. The repetition rate can be used to adjust the power and by optimizing the resonance it is possible to obtain high frequency semi-sinusoidal waveform. A typical measured output voltage of the employed pulsed power supply is depicted in Fig. 4.

The first portion of the output voltage waveform is the resonant circuit dominated by the magnetizing inductance of the transformer and the capacitances of the transformer and DBD. The period of this signal is approximately 11.2 µs. The second one is the resonance happening during the switches off-state between the leakage inductance and the capacitances of the transformer and DBD. The period of this signal is equal to 88.8µs. As can be seen from the figure the repetition rate is set to 10 kHz. It is quite important to generate symmetrical waveform regarding to clearing charge purpose and avoiding transformer saturation.

Fig. 5 shows the experimental hardware setup for the pulsed power supply. Here 1200V IGBT modules, SK75GB123, are used as power switches. Semikron Skyper 32-pro gate drive modules are utilized to drive the IGBTs and provide the necessary isolation between the switching-signal ground and the power ground. A Texas Instrument TMS320F28335 DSC (Digital Signal Controller) is used for PWM signal generation. A centre-tapped step-up transformer with an UU100 core 3C90 grade material ferrite from Ferroxcube, are designed with NA = NB = 5 and NS = 293. Here a 470pF capacitor (C_S) is placed across each switch to protect them against the voltage spikes. The output voltage is measured and captured using a Pintek DP-22Kpro differential probe and RIGOL DS1204B oscilloscope, respectively.

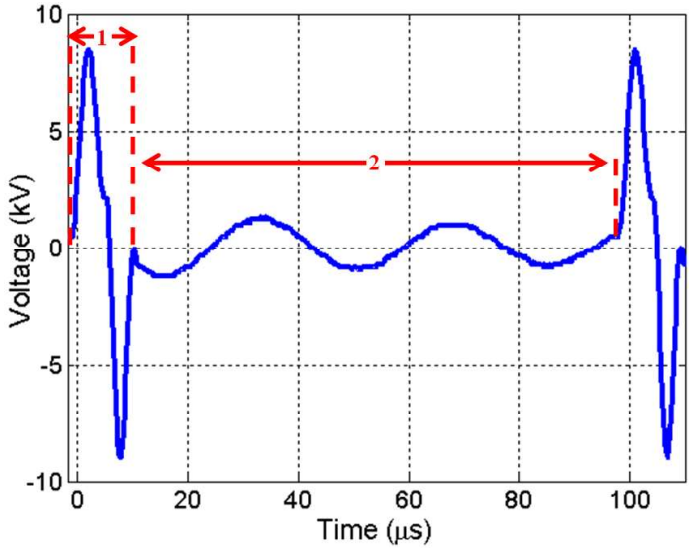

Fig. 4. A typical measured output voltage of the employed pulsed power supply.

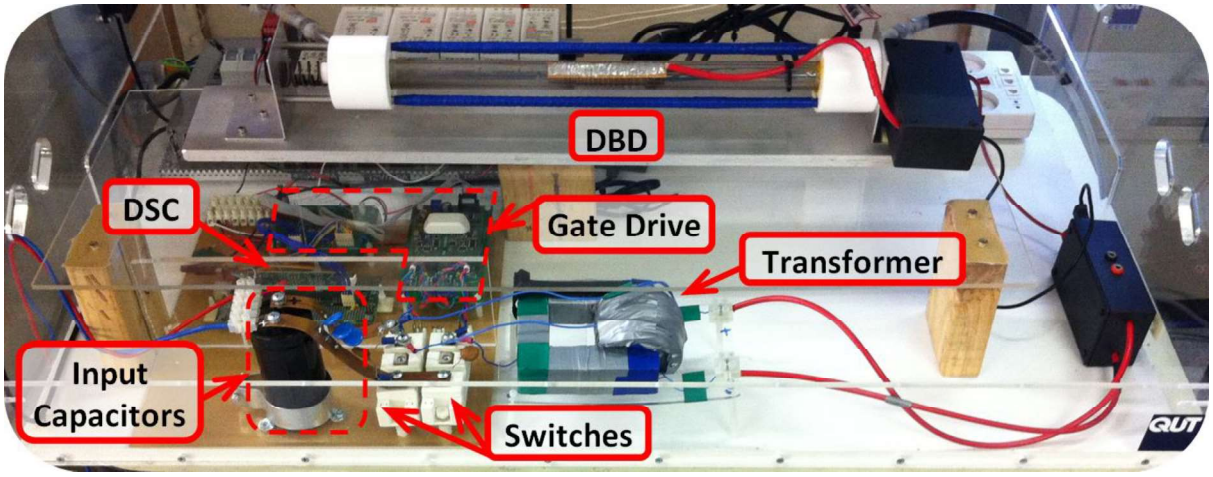

Fig. 5. Electrical Hardware setup with the DBD load.

III. Results and Discussion

A. Plasma effect on PM Size Distribution

The effect of plasma on emission treatment is considered for varied experiments based on the aforementioned Cummins diesel engine. In all experiments engine speed and load are kept constant at 40 kW (25 %load) and 2000 rpm, respectively. A portion of raw exhaust gas directly from an iso-kinetic sampling port of the tailpipe was diluted with air and passed through the reactor. Emissions concentration is measured before and after applying high voltage pulse to study the plasma effects. In addition, the median particle diameter which is another useful parameter to study the effect of plasma technique is also measured. It is to be noted that all illustrated results in each experiment have been obtained as an average over three consecutive measurements.

The experiments were made by applying output voltage from 10kVpp up to 19.44kVpp. However, the first effects of plasma was appeared at 15kVpp following with optimum operation at 17kVpp and finally high amount of small particle generation at 19.44kVpp. Hence, the measurements are reported in this section regarding to the mentioned three applied voltage levels. Fig. 6 illustrates the measured results. The applied output voltages across the DBD load for three different voltage levels of 15kVpp, 17kVpp, and 19.44kVpp are depicted in Fig. 6a. The measured output voltages show the rate of voltage rise of 2840V/µs.

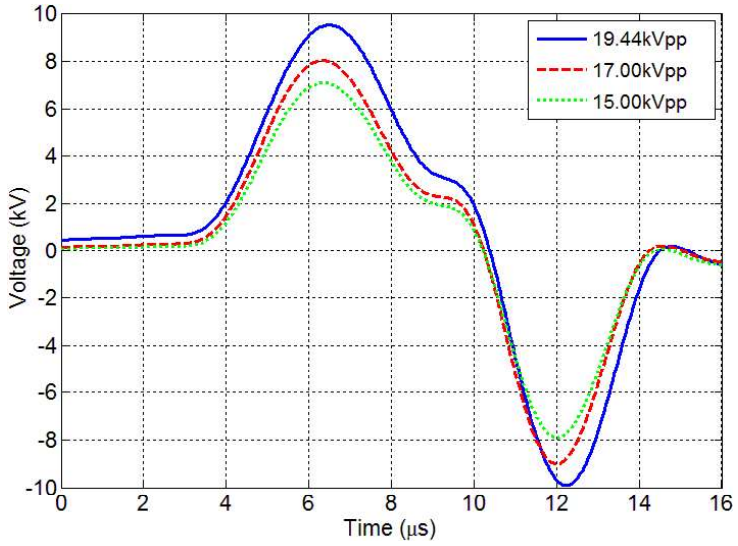

(a)

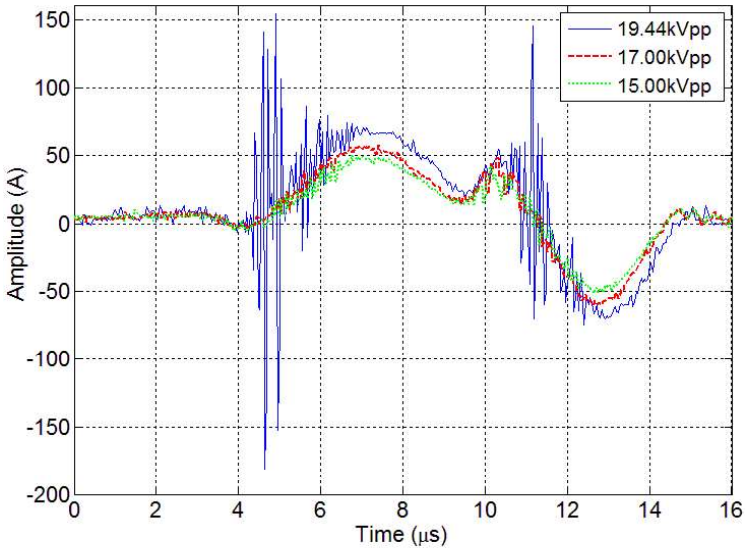

(b)

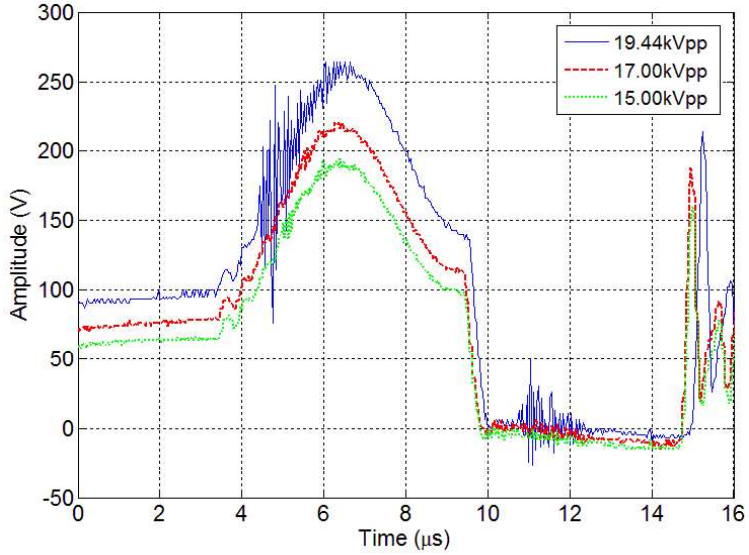

(c)

Fig. 6. The measured electrical parameters: a) output voltages across the DBD load, b) output current, and c) voltage stress across the switch.

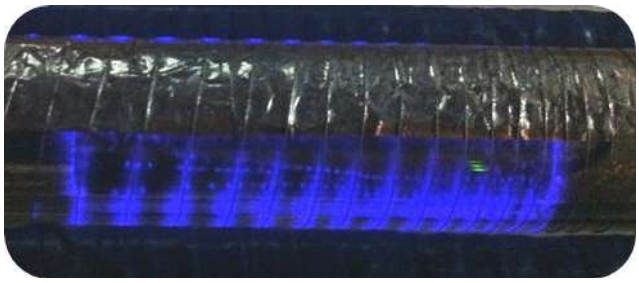

Fig. 7. DBD image.

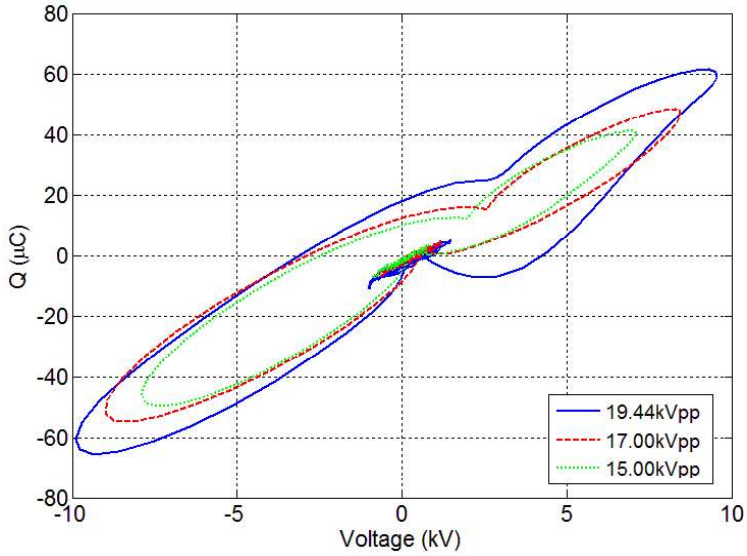

Fig. 8. V-Q cyclogram of the DBD load as a basis of power consumption calculation.

The measured load currents are illustrated in Fig. 6b, which shows many narrow pulsed current spikes occurring in each half-cycle of the applied voltage. The measured current at 19.44kVpp comparing with the other applied voltages shows higher number of the micro-discharges in the gap with much higher amplitude. This is due to the fact that the applied voltage has reached to the value of the breakdown voltage, which depends on the gap distance, dielectric material, repetition rate, and etc. Controlling the amplitude of current discharges is quite important as it can directly affect the plasma reaction which is discussed further. Fig. 6c shows the voltage stress across the switch during the switching transition. As can be seen, due to employing a centre-tapped transformer, the peak-to-peak voltage stress across the switch in a push-pull inverter is approximately two times of the input voltage.

In these experiments, the output voltage amplitude is controlled by changing the input DC voltage between 72.4 V, 84.4 V, and 94.8 V. Under same situation, Fig. 7 shows an image of DBD recorded at 19.44kVpp. As can be seen, NTP is clearly occurring between the two electrodes.

To measure the power consumption of the DBD load, the energy transferred to the DBD load has been calculated by employing the Lissajous (V−Q) diagram [51, 52].To measure Q a 4nF capacitor is placed in series with the DBD reactor. Thus, by measuring the voltage across the capacitor and multiplying it by its capacitance value it is possible to calculate Q. The energy consumed by the DBD reactor for one cycle is calculated from the area of V−Q curve for different experiments, where V is the measured voltage across the DBD reactor (see Fig. 8). Hence, by considering the employed repetition rate (frequency) it is possible to calculate the average consumed power by the DBD load. It is to be noted that the series connected capacitor is selected large enough to not to affect the DBD reactor capacitance. The relevant equations are:

$$W = \oint Q(t)dv \tag{2}$$

$$C(t) = \frac{dQ(t)}{dV(t)} \tag{3}$$

By substituting (3) in (2):

$$W = \oint \frac{Q(t)}{C} dQ = \frac{1}{2} CV^2 \tag{4}$$

Therefore, considering (2) to (4) the averaged consumed power can be calculated as below:

$$P_A = f \times W = f \oint Q(t)dv = f \frac{1}{2} CV^2 \tag{5}$$

The illustrated data in Fig. 8 clearly indicate that the DBD reactor power consumption correspondingly increases with the applied voltage level. This can be also realized from (5), which shows the relation between the power and the applied voltage. The calculated averaged power consumption (P_A) for the applied voltages of 15kVpp, 17kVpp, and 19.44kVpp are 27.37W, 36.54W, and 55.17W respectively. The higher averaged power at 19.44kVpp can be realized through the measured discharged current as it has occurred at higher amplitude and higher number of the micro-discharges.

In the first experiment, the maximum voltage level (19.44kVpp) is applied. To estimate the deposition rate on the reactor surface, emissions in the reactor inlet (reactor inlet no pulse) and reactor outlet (reactor outlet no pulse) without applying any pulse voltage are measured. Finally, the pulsed power supply is applied across the DBD and the emissions in reactor

outlet are measured (reactor outlet with pulse). The same process is employed in all following experiments.

Fig. 9 illustrates the particle size distribution at 19.44kVpp. There is a considerable amount of PM deposition on reactor surface which is likely related to small gap between the tubes (1mm). The median diameter in the reactor inlet is 70 nm, while in the reactor outlet is decreased to 66 nm. This shows that larger particles deposited more on the reactor surface. By applying pulsed power, as shown in this figure, the median diameter decreases remarkably to 35 nm. This implies that lots of big particles have been oxidized or broken to small particles by producing plasma inside the exhaust gasses at this voltage level.

The peak value of particle number at the reactor inlet is around $3.5\times10^7\ particle/cm^3$. This value declines to $1.2\times10^7\ particle/cm^3$ at the reactor outlet due to deposition. By applying pulsed power the graph peaks to $4.5\times10^7\ particle/cm^3$ which is approximately four times bigger than the particle number at reactor outlet without any pulse. The number of particles with diameter of less than 70 nm in the reactor outlet with applying pulse is higher than the particle numbers at the reactor outlet without any pulse. This effect increases even more at particle diameters less than 50 nm. At this level, the particle number at reactor outlet surpasses the number of particles at reactor inlet. These findings imply that, applying 19.44kVpp pulses at 10 kHz, increases the number of small particles considerably. The origin and nature of these particles is still not clear and will be of interests in future investigations. However, the effect of 19.44kVpp on particle size can be understood regarding to the high level of micro-discharges in the discharged current as depicted in Fig. 6b.

The effect of voltage level with 17kVpp is considered in the second experiment. The results obtained have been summarized in Fig. 10. The figure shows the median diameter changes from 70 nm at reactor inlet to 78 nm at reactor outlet without any pulse, and then falls to 75 nm at reactor outlet by applying pulse. This shows that the larger particles are deposited and also removed by plasma selectivity compared to smaller particles. As can be seen, at this voltage level (17kVpp) the number of small particles has not increased. This is an important feature in comparison with the previous experiment (19.44kVpp).

The last experiment is conducted by applying 15kVpp pulses. The measured results are depicted in Fig. 11, which shows no growth in the number of small particles as well as second experiment (17kVpp). The maximum of PM concentration took place at around 71 nm. There is a small difference between PM concentrations with and without applying plasma. Therefore, this voltage level can remove particles at the same rate of deposition.

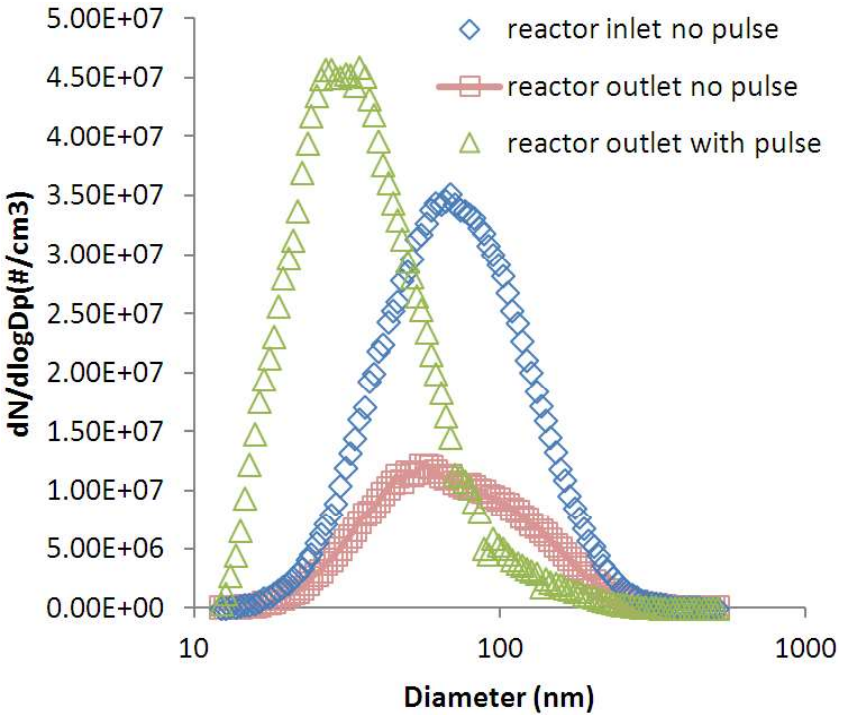

Fig. 9. Particle Size Distribution (2000rpm, 25%Load, 19.44kVpp).

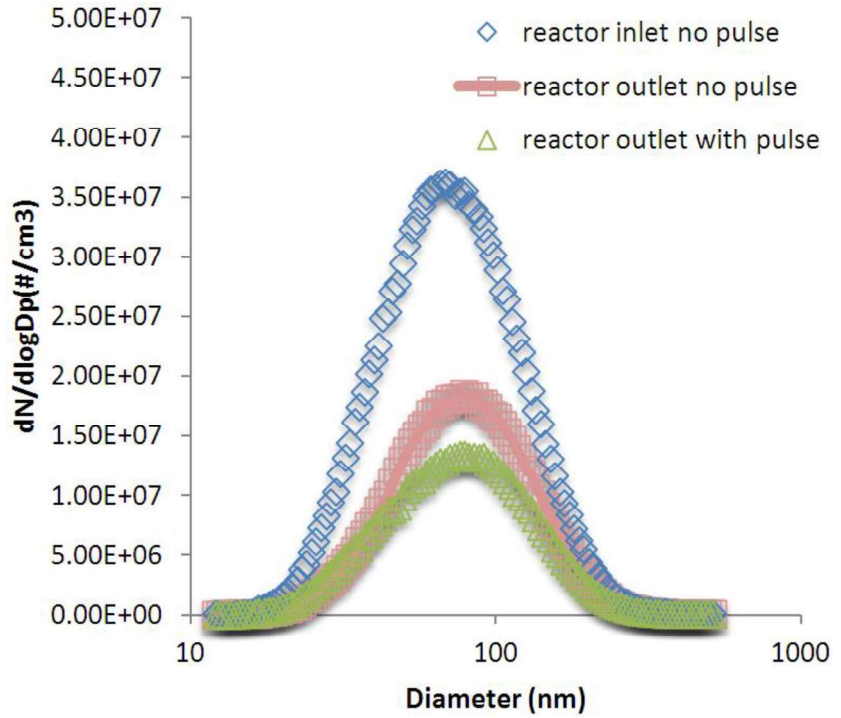

Fig. 10. Particle Size Distribution (2000rpm, 25%Load, 17kVpp).

Comparing the values of median diameter in the reactor inlet and outlet shows that the smaller particles are more likely to be deposited inside the reactor under the no pulse condition. On the other hand, by applying the high voltage pulse the median diameter is in same range of reactor inlet. There is no increase in the number of small particles at this

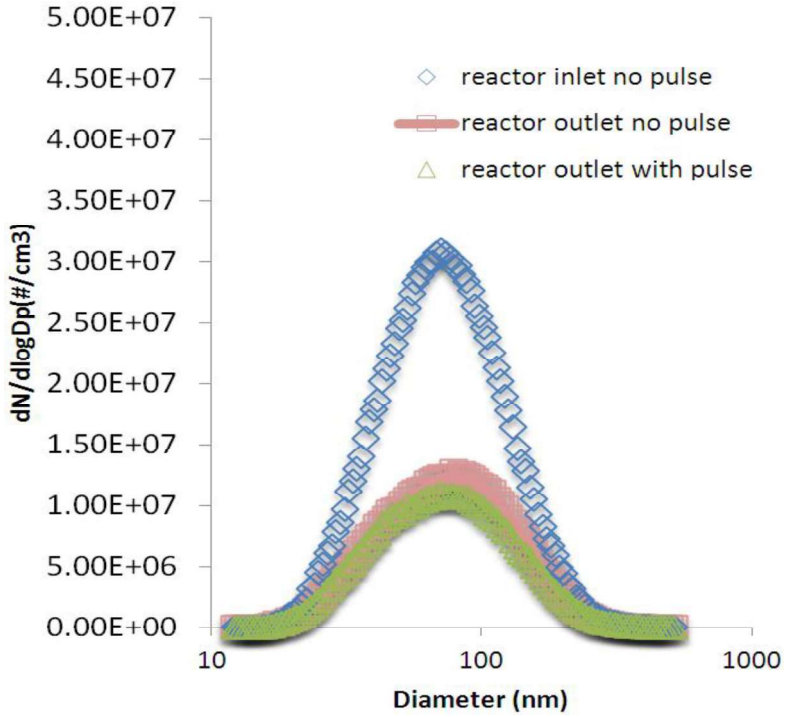

Fig. 11. Particle Size Distribution (2000rpm, 25%Load, 15kVpp).

voltage level. This trend in median diameter variation is almost in complete agreement with the voltage of 17kVpp.

Careful comparison of the reactor outlet particle size distribution, when there is no pulsed power, indicates that the distribution in Fig. 9 shows a reduction in particle median diameter, whereas Fig. 10 shows a slight increase in particle median diameter. Experiments for Fig. 10 were conducted approximately 30 min after that of Fig. 9. Therefore, there is a possibility that wall initial deposition occurred with larger particles and the later experiments for Fig. 10 favoured slightly smaller particles due to the larger surface area of the wall and the attraction of particles to deposited particles rather than the quartz wall alone.

B. PM removal efficiency

PM removal can be calculated based on the following equation:

$$PM\,removal = \frac{inlet\,PM\,concentration - outlet\,PM\,concentration\,(with\,pulse)}{inlet\,PM\,concentration} \times 100 \qquad (6)$$

Where the PM concentration unit is (particle/cm3) and PM removal is calculated for all PM diameters. Fig. 12 illustrates the PM removal at 19.44kVpp. PM deposition on the reactor surface increases with the PM size and gets to the maximum value of 70% removal at around 80 nm. But below 80nm PM removal decreases again. For most of the particle sizes, PM deposition on the reactor surface is more than 40%. When a 19.44kVpp voltage is applied to

the reactor, PM removal efficiency reaches the value of 90% for larger particles. Removal efficiency for particulate matter less than 80 nm is less than PM removal without applying any pulse. This indicates undesirable operation of the plasma within this particle size range. Also there is no removal for particles smaller than 50 nm. There is a high possibility that this incense in particle numbers can be related to the following two factors: firstly, fragmentation of larger particles by electron impact reactions or incomplete oxidation and secondly, oxidation of gaseous exhaust emissions to particles by plasma generated ozone.

Fig. 13 shows the PM removal at 17kVpp which shows that PM removal by plasma is more effective than deposition removal. This means that at this level of voltage, all deposited particles and also some large particles inside the flow can be removed or oxidized. For particles smaller than 35nm, PM removal percentage by deposition is higher than PM removal by plasma. Apparently, smaller particles cannot be removed by plasma within this range (<35nm). However another possibility can be dissociation of larger particles to smaller ones by electron impact reactions.

PM removal efficiency at 15kVpp is illustrated in Fig. 14. As can be seen the PM removal for both graphs increases to an optimum value then decreases. The maximum PM removals in reactor outlet with and without the pulse are 61% and 69% respectively. For particles larger than the 60 nm diameter, PM removal when applying pulsed power is slightly higher than PM removal without any pulse. However, for particles with smaller diameters, these values are in the same ranges.

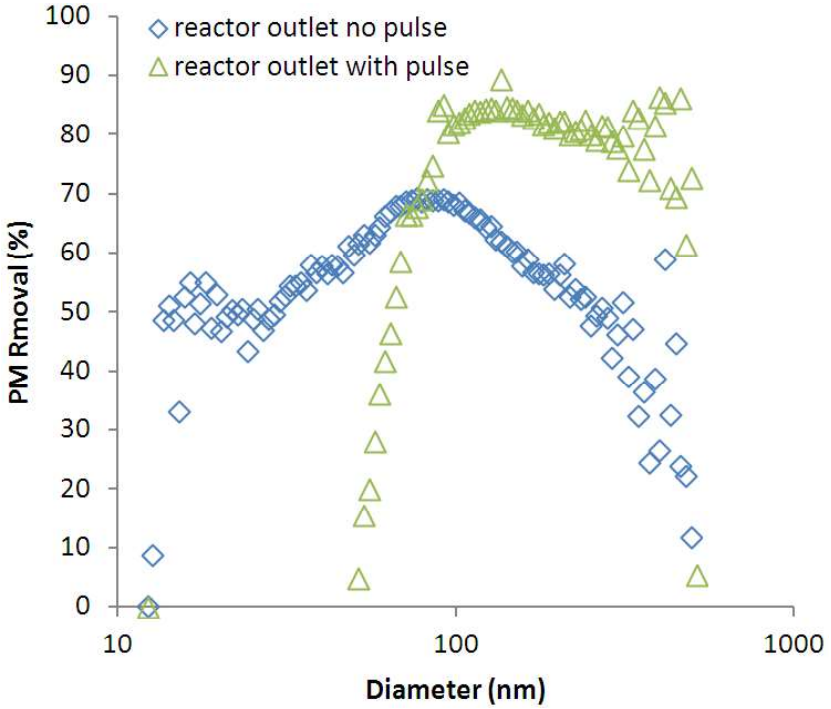

Fig. 12. PM removal as a function of PM size (2000rpm, 25%Load, 19.44kVpp)

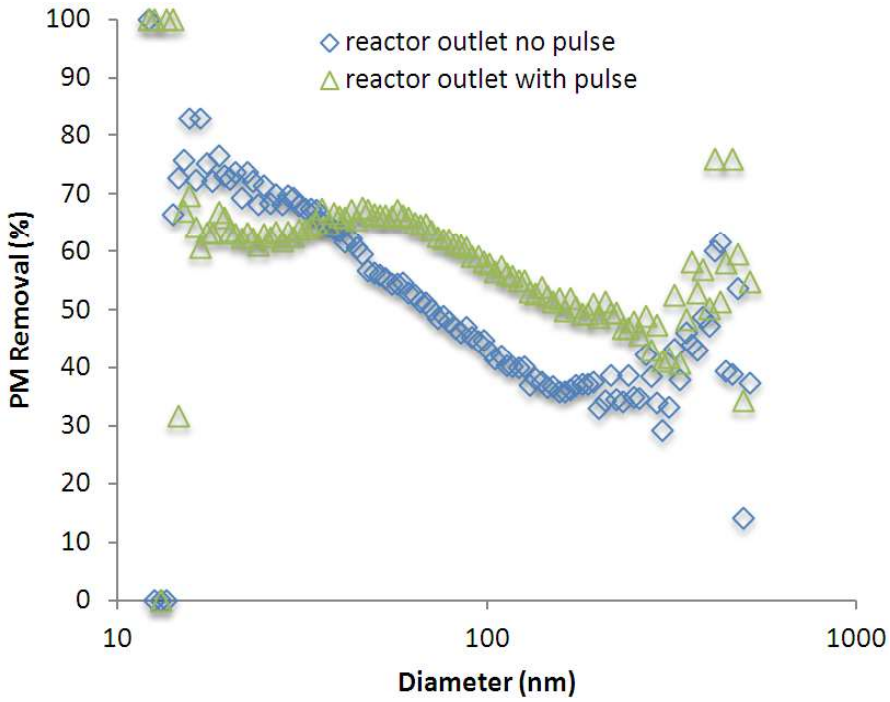

Fig. 13. PM removal as a function of PM size (2000rpm, 25%Load, 17kVpp)

Regarding the results obtained, it can be concluded that the voltage level has an important role in the size dependent removal efficiency. At 15kVpp the particle size distribution has been affected slightly. The PM removal without producing small particles can be improved as the voltage increases to 17kVpp. The increase in the number of small particles has been noticed when the voltage level goes up to 19.44kVpp, while larger particles have been reduced considerably. By taking into account all the above mentioned features, the experiment with 17kVpp voltage shows better efficiency in terms of particle size distribution for the given configuration.

C. Plasma Effect on PM Mass Reduction

After studying the effect of different voltages on particle size distribution, in this section, the effect of plasma on particle mass reduction is considered. In a similar way to the previous sections three different voltage levels have been applied to the DBD load. All results obtained have been summarized in Table I. PM mass concentrations in the reactor inlet were 4.56 ($\frac{mg}{m^3}$), 4.26 ($\frac{mg}{m^3}$) and 5.14 ($\frac{mg}{m^3}$) respecting to the variation of engine operating conditions for the three tests conducted. These values decreased to 2.84 ($\frac{mg}{m^3}$), 3.68 ($\frac{mg}{m^3}$) and 4.37 ($\frac{mg}{m^3}$) at reactor outlet in the no pulse condition, respectively. This shows a significant particle deposition inside the reactor. When the pulsed power is applied, plasma PM removal

occurred. This causes the PM mass concentration reduction of 43.9 %, 38.6% and 27.1% at 19.44kVpp, 17kVpp and 15kVpp, respectively.

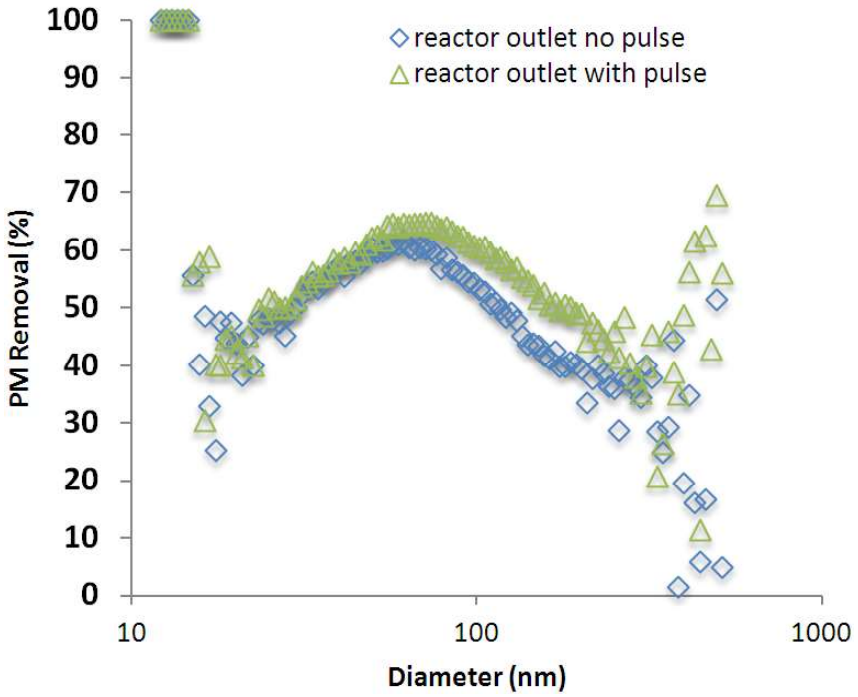

Fig. 14. PM removal as a function of PM size (2000rpm, 25%Load, 15kVpp)

TABLE I
PM MASS REDUCTION AT DIFFERENT VOLTAGE LEVELS

Applied Voltage / Measurement	19.44kVpp	17kVpp	15kVpp
Reactor Inlet PM Concentration ($\frac{mg}{m^3}$)	4.56	4.26	5.14
Reactor Outlet No Pulse PM Concentration($\frac{mg}{m^3}$)	2.84	3.68	4.37
Reactor Outlet By-Pulse PM Concentration ($\frac{mg}{m^3}$)	2.56	2.62	3.74
Plasma PM Mass Removal Efficiency (%)	43.9	38.6	27.1

The maximum PM mass reduction has been obtained when the voltage level is 19.44kVpp. However, according to the particle size distribution measurements, this voltage level increases the number of small particles, which is not a desirable feature. The 17kVpp applied voltage shows a more suitable performance with good mass reduction of around 40% without any increase in ultra-fine particle numbers. The 15kVpp voltage level is found to be almost a threshold for the given configuration, below which no significant PM mass reduction, PM removal, and PM size distribution which have not been affected too much.

IV. Conclusion

In this study the effect of non-thermal plasma obtained by applying high voltage pulses on PM size distribution and PM mass reduction were investigated. It was found that NTP plasma not only affects the PM mass concentration, but also changes the PM size distribution. At very high voltage levels (here 19.44kVpp), NTP was very effective for PM mass reduction. However, PM mass reduction is not the only concern. It became clear that at high voltage levels the number of ultra-fine particles increases significantly. Regarding the negative health effects of tiny particles, the performance of plasma at such a high voltage levels is not desirable. Considering the PM mass reduction and PM size distribution simultaneously, an optimum voltage level of 17kVpp at 10 kHz was found for the given configuration and operating condition. Moreover the wall attachments of particulates are another important parameter which should be considered in all experiments. It was found that wall attachments are variable even without introducing any plasma. Therefore, particle deposition insides the reactor and its effect on plasma PM removal should be considered with more details in future.

References

[1] C.-L. Song, F. Bin, Z.-M. Tao, F.-C. Li, and Q.-F. Huang, "Simultaneous removals of NOx, HC and PM from diesel exhaust emissions by dielectric barrier discharges," *Journal of Hazardous Materials,* vol. 166, pp. 523-530, 2009.

[2] A. Chaloulakou, M. I, and G. I, "Compliance with the annual NO2 air quality standard in Athens. Required NOx levels an expected health implications," *Atmos Environ,* vol. 42, pp. 454–465, 2008.

[3] A. Mayer, H. Egli, J. Burtscher, T. Czerwinski, and D. Gehrig, "Particle size distribution downstream traps of different design," *SAE* vol. Paper No. 950373 1995.

[4] L. Zhua, J. Yu, and X. Wang, "Oxidation treatment of diesel soot particulate on CexZr1−xO2, ," *J. Hazard. Mater,* vol. 140, pp. 205-210, 2007.

[5] Oberdörster G, Sharp Z, Atudorei V, Elder A, Gelein R, Kreyling W*, et al.*, "Translocation of inhaled ultrafine particles to the brain," *Inhalation Toxicology,* vol. 16, pp. 437–45, 2004.

[6] T. Matsumoto, D. Wang, T. Namihira, and H. Akiyama, "Energy Efficiency Improvement of Nitric Oxide Treatment Using Nanosecond Pulsed Discharge," *Plasma Science, IEEE Transactions on,* vol. 38, pp. 2639-2643, 2010.

[7] K. Takaki, M. A. Jani, and T. Fujiwara, "Removal of nitric oxide in flue gases by multi-point to plane dielectric barrier discharge," *Plasma Science, IEEE Transactions on,* vol. 27, pp. 1137-1145, 1999.

[8] A. Mizuno, "Industrial applications of atmospheric non-thermal plasma in environmental remediation," *Plasma Physics and Controlled Fusion,* vol. 49, p. A1, 2007.

[9] M. Saito, H. Hoshino, T. Furuhata, and M. Arai, "Continuous regeneration of an electrically heated diesel particulate trap: Mechanism of particulate matter trapping and improvement of trapping efficiency," *International Journal of Engine Research,* vol. 11, pp. 127-136, April 1, 2010 2010.

[10] Plasma Exhaust Treatment [Online]. Available: http://www.dieselnet.com/tech/plasma.html

[11] P. Davari, F. Zare, and A. Ghosh, "A flexible solid-state pulsed power topology," in *Power Electronics and Motion Control Conference (EPE/PEMC), 2012 15th International*, 2012, pp. DS2b.12-1-DS2b.12-6.

[12] P. Davari, F. Zare, A. Ghosh, and H. Akiyama, "High-Voltage Modular Power Supply Using Parallel and Series Configurations of Flyback Converter for Pulsed Power Applications," *Plasma Science, IEEE Transactions on,* vol. 40, pp. 2578-2587, 2012.

[13] S. Zabihi, F. Zare, G. Ledwich, A. Ghosh, and H. Akiyama, "A Novel High-Voltage Pulsed-Power Supply Based on Low-Voltage Switch-Capacitor Units," *Plasma Science, IEEE Transactions on,* vol. 38, pp. 2877-2887, 2010.

[14] A. A. El-Deib, F. Dawson, S. Bhosle, and G. Zissis, "Circuit-Based Model for a Dielectric Barrier Discharge Lamp Using the Finite Volume Method," *Plasma Science, IEEE Transactions on,* vol. 38, pp. 2260-2273, 2010.

[15] S. Tao, Z. Dongdong, Y. Yang, Z. Cheng, W. Jue, Y. Ping*, et al.*, "A Compact Repetitive Unipolar Nanosecond-Pulse Generator for Dielectric Barrier Discharge Application," *Plasma Science, IEEE Transactions on,* vol. 38, pp. 1651-1655, 2010.

[16] B. Rahmani, S. Bhosle, and G. Zissis, "Dielectric-Barrier-Discharge Excilamp in Mixtures of Krypton and Molecular Chlorine," *Plasma Science, IEEE Transactions on,* vol. 37, pp. 546-550, 2009.

[17] K. Takaki, M. Shimizu, S. Mukaigawa, and T. Fujiwara, "Effect of electrode shape in dielectric barrier discharge plasma reactor for NOx removal," *Plasma Science, IEEE Transactions on,* vol. 32, pp. 32-38, 2004.

[18] N. Osawa and Y. Yoshioka, "Generation of low-frequency homogeneous dielectric barrier discharge at atmospheric pressure," *Plasma Science, IEEE Transactions on,* vol. 40, pp. 2-8, 2012.

[19] H. Ghomi, N. N. Safa, and S. Ghasemi, "Investigation on a DBD Plasma Reactor," *Plasma Science, IEEE Transactions on,* vol. 39, pp. 2104-2105, 2011.

[20] H. Ayan, G. Fridman, A. F. Gutsol, V. N. Vasilets, A. Fridman, and G. Friedman, "Nanosecond-Pulsed Uniform Dielectric-Barrier Discharge," *Plasma Science, IEEE Transactions on,* vol. 36, pp. 504-508, 2008.

[21] H. Piquet, S. Bhosle, R. Diez, and M. V. Erofeev, "Pulsed Current-Mode Supply of Dielectric Barrier Discharge Excilamps for the Control of the Radiated Ultraviolet Power," *Plasma Science, IEEE Transactions on,* vol. 38, pp. 2531-2538, 2010.

[22] T. Yamamoto, M. Okubo, K. Hayakawa, and K. Kitaura, "Towards ideal NO x control technology using plasma-chemical hybrid process," Phoenix, AZ, USA, 1999, pp. 1495-1502.

[23] B. S. Rajanikanth and S. Rout, "Studies on nitric oxide removal in simulated gas compositions under plasma-dielectric/catalytic discharges," *Fuel Processing Technology,* vol. 74, pp. 177-195, 2001.

[24] V. Ravi, Y. S. Mok, B. S. Rajanikanth, and H. C. Kang, "Temperature effect on hydrocarbon-enhanced nitric oxide conversion using a dielectric barrier discharge reactor," *Fuel Processing Technology,* vol. 81, pp. 187-199, 2003.

[25] B. S. Rajanikanth and V. Ravi, "Removal of nitrogen oxides in diesel engine exhaust by plasma assisted molecular sieves," *Plasma Science and Technology,* vol. 4, pp. 1399-1406, 2002.

[26] T. Yamamoto, B. S. Rajanikanth, M. Okubo, T. Kuroki, and M. Nishino, "Performance evaluation of nonthermal plasma reactors for NO oxidation in diesel engine exhaust gas treatment," *IEEE TRANSACTIONS ON INDUSTRY APPLICATIONS,* vol. 39, pp. 1608-1613, 2003.

[27] B. S. Rajanikanth and B. R. Sushma, "Injection of N-radicals into diesel engine exhaust treated by plasma," *Plasma Science and Technology,* vol. 8, pp. 202-206, 2006.

[28] A. D. Srinivasan and B. S. Rajanikanth, "Nonthermal-plasma-promoted catalysis for the removal of NOX from a stationary diesel-engine exhaust," *IEEE TRANSACTIONS ON INDUSTRY APPLICATIONS,* vol. 43, pp. 1507-1514, 2007.

[29] A. D. Srinivasan, B. S. Rajanikanth, and S. Mahapatro, "CORONA TREATMENT FOR NOX REDUCTION FROM STATIONARY DIESEL ENGINE EXHAUST IMPACT OF NATURE OF ENERGIZATION AND EXHAUST COMPOSITION," 2009.

[30] V. Ravi, Y. S. Mok, B. S. Rajanikanth, and H. C. Kang, "Studies on nitrogen oxides removal using plasma assisted catalytic reactor," *Plasma Science and Technology,* vol. 5, pp. 2057-2062, 2003.

[31] B. S. Rajanikanth, A. D. Srinivasan, and B. A. Nandiny, "A cascaded discharge plasma-adsorbent technique for engine exhaust treatment," *Plasma Science and Technology,* vol. 5, pp. 1825-1833, 2003.

[32] B. S. Rajanikanth, S. Das, and A. D. Srinivasan, "Unfiltered Diesel Engine Exhaust Treatment by Discharge Plasma: Effect of Soot Oxidation," *Plasma Science & Technology,* vol. 6, pp. 2475-2480, 2004.

[33] B. S. Rajanikanth and V. Ravi, "DeNOx study in diesel engine exhaust using barrier discharge corona assisted by v2O5/TiO2 catalyst," *Plasma Science and Technology,* vol. 6, pp. 2411-2415, 2004.

[34] B. S. Rajanikanth and A. D. Srinivasan, "Pulsed plasma promoted adsorption/catalysis for NOx removal from stationary diesel engine exhaust," *IEEE Transactions on Dielectrics and Electrical Insulation,* vol. 14, pp. 302-311, 2007.

[35] A. D. Srinivasan and B. S. Rajanikanth, "Pulsed plasma treatment for NOx reduction from filtered/unfiltered stationary diesel engine exhaust," New Orleans, LA, 2007, pp. 1893-1900.

[36] B. S. Rajanikanth, D. Sinha, and P. Emmanuel, "Discharge plasma assisted adsorbents for exhaust treatment: A comparative analysis on enhancing NOx removal," *Plasma Science and Technology,* vol. 10, pp. 307-312, 2008.

[37] B. S. Rajanikanth, S. Mohapatro, and L. Umanand, "Solar powered high voltage energization for vehicular exhaust cleaning: A step towards possible retrofitting in vehicles," *Fuel Processing Technology,* vol. 90, pp. 343-352, 2009.

[38] G. A. Stratakis, "Experimental investigation of catalytic soot oxidation and pressure drop characteristics in wall flow diesel particulate filters,," Ph.D. Thesis, University of Thessaly, Greece., 2004.

[39] V. Ramanathan, "Global dimming by air pollution and global warming by greenhouse gases," *Nucleation and Atmospheric Aerosols* vol. 6, pp. 473-483, 2007

[40] A. Seaton, W. MacNee, D. K, and D. Godden, " Particulate air pollution and acute health effects," *Lancet,* vol. 345, pp. 176-178., 1995.

[41] A. Sydbom, A. Blomberg, S. Parnia, N. Stenfors, T. Sandstrom, and S. E. Dahlen, "Health effects of diesel exhaust emissions," *Eur respir J* vol. 17, pp. 733-746, 2001.

[42] C. M. omers, B. E. McCarry, F. Malek, and J. S. Quinn, " Reduction of particulate air pollution lowers the risk of heritable mutations in mice," *Science* vol. 304, pp. 1008–1010, 2004.

[43] W. A. Majewski. Diesel exhaust particle size [Online]. Available: http://www.dieselnet.com/tech/dpm_size.html
[44] R. O. McClellan, "Health Effects of Exposure to Diesel Exhaust Particles," *Ann. Rev. Pharmacol. Toxicol,* vol. 27, pp. 279-300, 1989.
[45] J. H. Seinfeld, *Air pollution: Physical and chemical fundamentals*. New York: McGraw-Hill, Inc., 1975.
[46] D. B. Kittelson, "Engines and nanoparticles: A review," *J. Aerosol Sci.,* vol. 29, pp. 575-588, 1998.
[47] W. A. Majewski. Diesel particulate matter [Online]. Available: http://www.dieselnet.com/tech/dpm.html
[48] A. Peters, H. E. Wichmann, T. Tuch, J. Heinrich, and J. Heyder, "Respiratory effects are associated with the number of ultrafine particles," *American journal of respiratory and critical care medicine,* vol. 155, pp. 1376-1383, 1997.
[49] N. C. Surawski, Z. D. Ristovski, R. J. Brown, and R. Situ, "Gaseous and particle emissions from an ethanol fumigated compression ignition engine," *Energy Conversion and Management,* vol. 54, pp. 145-151, 2012.
[50] Z. D. Ristovski, B. Miljevic, N. C. Surawski, L. Morawska, K. M. Fong, F. Goh, *et al.*, "Respiratory health effects of diesel particulate matter," *Respirology,* vol. 17, pp. 201-212, 2012.
[51] J. Kriegseis, S. Grundmann, and C. Tropea, "Power consumption, discharge capacitance and light emission as measures for thrust production of dielectric barrier discharge plasma actuators," *Journal of Applied Physics,* vol. 110, pp. 013305-9, 07/01/ 2011.
[52] R. P. Mildren and R. J. Carman, "Enhanced performance of a dielectric barrier discharge lamp using shortpulsed excitation," *J. Phys. D.: Appl. Phys.,* vol. 34, pp. L1-L6, Jan. 2001.

Meisam Babaie received his B.S. degree in fluid mechanical engineering from Shahrood University of Technology and M.S. degree in energy systems engineering from K.N.Toosi University of Technology in 2005 and 2008, respectively. He is currently pursuing his Ph.D. in the school of Chemistry, Physics and Mechanical Engineering at Queensland University of Technology, Brisbane, Australia. His main research interests include biofuels, emission reduction, thermo-economic and exergy analysis of energy systems, optimization, and numerical modelling.

Pooya Davari (S'11-M'13) received his B.S. and M.S. degrees both in electronic engineering and his PhD degree in Power Electronics in 2004, 2008, and 2013, respectively. Currently, he is a lecturer at Queensland University of Technology, Brisbane, Australia. His main research interests include pulsed power, power electronics topologies and control techniques, and intelligent signal processing.

Firuz Zare (M'97–SM'06) received his BSc (Eng) degree in Electronic Engineering, his MSc degree in Power Engineering and his PhD degree in Power Electronics in 1989, 1995 and 2001, respectively. He spent several years in industry as a team leader and development engineer where he was involved in electronics and power electronics projects. He was with Queensland University of Technology as an Associate Professor. He is currently holding a Lead Engineer position with Danfoss Power Electronics, Denmark. His main research interests include Problem-Based Learning in Power Electronics, Power Electronics Topologies and Control, Pulse Width Modulation Techniques, EMC/EMI in Power Electronics and Renewable Energy Systems.

MD Mostafizur Rahman received his B.S.C in Mechanical engineering from Rajshahi University of Engineering and Technology (RUET), Bangladesh .He then worked as a lecturer in the same university for three years. He is currently pursuing his Ph.D. in the school of Chemistry, Physics and Mechanical Engineering at Queensland University of Technology, Brisbane, Australia. His main research interests include biofuels, diesel engine particle emission, and particle morphology etc.

Hassan Rahimzadeh received his BSc and MSc in Mechanical Engineering, West Virginia Inst. of Technology and West Virginia St. University (USA) and his PhD in Instrumentation Measurement, New South Wales University (Australia) in 1977, 1978 and 1986, respectively. He has been with Department of Mechanical Engineering, Amirkabir University of Technology (Iran) for several years. His main research interests are two phase flow (physical & numerical modelling), hydraulics structures, environmental pollution control, renewable energy and Instrumentation.

Zoran Ristovski received his BE in Electrical Engineering, his MSc degree and his PhD degree in Engineering Physics in 1988, 1993 and 1996, respectively, from Belgrade University. Since 1997 he moved to Australia were he had various academic appointments. He is currently a Professor with the Queensland University of Technology, Brisbane, Australia. His main research interests include the broad area of atmospheric aerosol science with a special focus on nanoparticle vehicle emissions.

Richard Brown received his BE(Hons) in Mechanical Engineering from the University of Technology Sydney, his BTh from the Sydney College of Divinity and his PhD degree in combustion from the University of Sydney in 1984, 1986 and 1996, respectively. He completed postdocs at the CSIRO Division of Atmospheric Research and at the Toyohashi University of Technology before joining the academic staff of the Queensland University of Technology in 2000. He is an Associate Professor whose main research interests are thermodynamics and fluid mechanics with a focus on renewable energy and emissions.